

See discussions, stats, and author profiles for this publication at: <http://www.researchgate.net/publication/262567499>

Mould taper optimization for continuous casting steels by numerical simulation

ARTICLE in CHINA FOUNDRY · APRIL 2010

Impact Factor: 0.43

CITATIONS

3

READS

40

8 AUTHORS, INCLUDING:



[Tongmin Wang](#)

Dalian University of Technology

119 PUBLICATIONS 371 CITATIONS

SEE PROFILE



[Zongning Chen](#)

Dalian University of Technology

33 PUBLICATIONS 130 CITATIONS

SEE PROFILE



[Zhiqiang Cao](#)

Dalian University of Technology

48 PUBLICATIONS 221 CITATIONS

SEE PROFILE

Mould taper optimization for continuous casting steels by numerical simulation

*Wang Tongmin, Cai Shaowu, Li Jun, Xu Jingjing, Chen Zongning, Zhu Jing, Cao Zhiqiang and Li Tingju

(School of Materials Science and Engineering, Dalian University of Technology, Dalian 116024, China)

Abstract: A transient, two-dimensional, coupled finite element model was employed to simulate the solidification and shrinkage of continuous casting steels by means of ANSYS. In the model, a gap-dependent heat transfer condition was introduced to modify the heat flux function, and the variations of material thermal properties, mechanical properties as well as the yield function with temperature were considered. The solidification and shrinkage processes of four round billets and two square billets were simulated by indirect coupled method. Simulation results show that carbon content, pouring temperature, casting speed and shape of billets have distinct influence on the solidification shrinkage of billets. Ideal continuous parabolic tapers were designed and optimized according to the calculated shrinkage curves of billets.

Key words: mould; parabolic taper; shrinkage; numerical simulation

CLC number: TG249.7/TP391.9

Document code: A

Article ID: 1672-6421(2010)01-061-07

Continuous casting technology is currently the primary method in production of steels billets and slabs. The mould is considered as the heart of continuous caster. Molten steel solidifies and shrinks in the mould, inevitably forming gaps, which is a restrictive condition in continuous casting, between the solidified shell and the mould's copper plate. The mould design should adapt to the heat shrinkage of the billets, therefore a converse taper was designed for the mould inner cavity to reduce the formed gap^[1], increase the thickness of the solidified shell, and to improve the casting speed and the surface quality of the billets, while, the mould can not only avoid and reduce the temperature recovery events^[2], but also is propitious to prevent billets from crack and distortion^[3]. In fact, continuous casting is operated at high temperature above the steel melting point, therefore, the measurement of temperature, stress and solidification shrinkage is almost impossible. A full-

scale physical simulation is also very difficult and expensive.

Based on intensive research on continuous casting, physical phenomena of heat transfer and stress-strain evolution can be described by model mathematically, which normally is represented by a set of differential or partial differential equations. Many scholars have done lots of studying work on heat transfer, metal solidification, and stress-strain evolution during continuous casting by the mathematical analysis. Thomas^[4] and Park^[5] have developed the finite element thermal stress to predict temperature, distortion and resultant stress in the mould of thin slab continuous casters. J. Z. Jin^[3] has developed a mathematical model for solidification in continuous casting by finite difference method. E. G. Wang^[6] has developed a finite element mathematical model to simulate the thermal elastoplastic stress on continuous casting billet in the mould so as to optimize and design the continuous casting mould taper. A. E. Huespe^[7] has used the plane strain with uniform axial strain to simulate mechanical behavior of the round and slab billets. Thomas, G. O'Connor and Jonathan A Dantzig^[8] have used the calibrated numerical simulation model to analyze continuous casting process and derived an ideal narrow face taper prediction equation. G. Ding^[9] has studied the solidification and shrinkage of continuous cast slab and the suggested optimized mould taper strategy is proved successful in the practical production. L. G. Zhu and R.V. Kumar^[10] have optimized the mould taper profile in order to intensify the heat transfer and improve the quality of the cast products by mathematical model. I. V. Samarasekera^[11] has designed the high speed billet mould taper by the industrial experiments and a mathematical billet thermal and solidification model.

*Wang Tongmin

Male, born in 1971, Ph.D. He gained his bachelor's and master's degree from Harbin Institute of Technology in 1995 and 1997, respectively, and the doctor's degree from Dalian University of Technology in 2000. He is presently a professor and doctoral supervisor in Dalian University of Technology. He has been worked as a post-doctor in Osaka University of Japan and in RWTH Aachen of Germany. His studies mainly focus on numerical simulation of metal solidification and in-situ observation on grain growth by synchrotron radiation imaging. His over 40 papers have been published in recent 5 years in journals domestic and abroad.

E-mail: tmwang@dlut.edu.cn

Received: 2009-03-15; Accepted: 2009-09-20

In this paper, the solidification and shrinkage for four round billets and two square billets were simulated. Rules of shell growth, shell temperature and stress-strain evolution and billet shrinkage were numerically studied. The mould taper was therefore optimized.

1 Simulation model

Two-dimensional finite element model was developed to predict the thermal-stress fields of molten steel within the mould. A heat flux varying with the distance from meniscus was employed at the boundary between the billet and mould. For the square billets, when the solidified shell appears in the corner, the heat flux suddenly decreased to only 1/3 of the standard value in the boundary center [12]. In the simulation process, temperature fields were computed first, and then the temperature results were transferred to the thermal-stress calculation model as initial condition.

1.1 Model fundamental

- (a) Ignore the longitudinal heat conduction in the direction of casting.
- (b) Ignore the heat transfer difference between inside and outside of curved mould.
- (c) Ignore the creep deformation of the solidified shell, but consider and develop elastic-plasticity model.
- (d) Assume that metal materials obey the Mises yield criterion.

The solidification with phase change and the temperature distribution inside the billet during the continuous casting of steel can be described by the two-dimensional non-steady-state heat conduction equation [13]:

$$\rho(T)c(T)\frac{\partial T}{\partial \tau} = \frac{\partial}{\partial x}(k(T)\frac{\partial T}{\partial x}) + \frac{\partial}{\partial y}(k(T)\frac{\partial T}{\partial y}) + S \quad (1)$$

Where $\rho(T)$ is the density of steel (kg/m^3), T is the temperature (K), τ is the time (s), x, y are the rectangular coordinates, $k(T)$ is the thermal conductivity ($\text{W/m}\cdot\text{k}$), $c(T)$ is the specific heat ($\text{J/kg}\cdot\text{k}$), and S is the latent heat source (W/m^3).

Latent heat was generated during the phase change between the liquidus and solidus temperatures and it can be expressed by the following equation:

$$S = \rho(T)_s L \frac{\partial f_s}{\partial \tau} \quad (2)$$

Where L is the latent heat of fusion (J/kg), $\rho(T)_s$ is the density of solid (kg/m^3), f_s is the solid fraction.

The increment total strain can be described by the following equation [6, 12]:

$$\{d\varepsilon\} = \{d\varepsilon\}_e + \{d\varepsilon\}_T + \{d\varepsilon\}_p \quad (3)$$

Where $\{d\varepsilon\}_e$, $\{d\varepsilon\}_p$, $\{d\varepsilon\}_T$ are the elastic, plastic and thermal strain, respectively.

1.2 Geometry mesh grid model and method of simulation

Due to the symmetry, the 1/4 entity model was selected for the calculation of both round and square billets. The mould length

was 780 mm (with working length of 700 mm), diameter of the round billet is 182 mm, the square billet section size is $165 \text{ mm} \times 165 \text{ mm}$ and the mould corner radius is 5 mm. Considering edge effect of heat transfer, the mesh grid of the model was small in the dense heat transfer regions, and gentle big mesh grid was used in other regions. Figure 1 and Fig. 2 show the mesh grid entity model pictures of round and square billets.

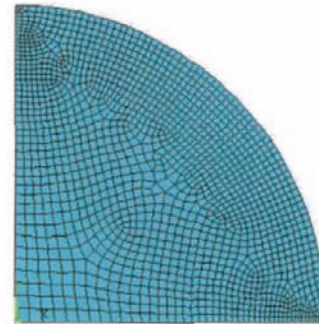


Fig. 1: Mesh grid entity model of round billets (1/4 symmetry)

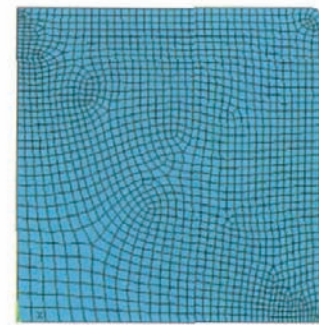


Fig. 2: Mesh grid entity model of square billets (1/4 symmetry)

The simulation method is explained in Fig. 3 by taking round billet as example. The fixed point P on the billet boundary goes through the whole mould from the meniscus to the bottom of mould. In the dynamic process of pulling billet, results of the transient temperature field were obtained first, and then the thermal results as initial conditions were transferred to the stress-strain calculation. The calculation process was done at every Δt or Δh , hence, the instantaneous solidification shrinkage information at point P can be gained during $t=0$ and $t=l/v$ (l is the working length, v the casting speed). It is easy to get the shrinkage curve at point P which can be referred to optimize the mould taper.

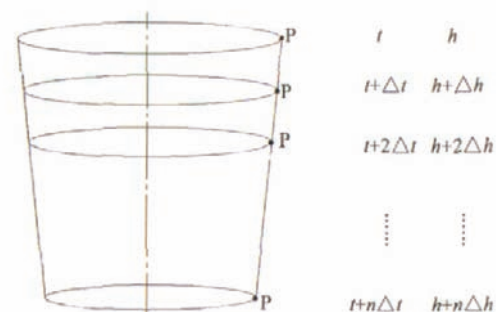


Fig. 3: Sketch of simulation method

1.3 Initial condition and boundary condition

Pouring temperature was selected as the initial temperature. Heat transfer between the billet and mould was defined by a function varying with the effect of shrinkage gap [5, 6, 7]. In the model, according to actual working condition and mould parameters, the modified heat flux function was loaded to the surface of the billet. The function is as follow [14, 15]:

$$q = 1.2 \times (2680 - 335 \times \sqrt{t}) \quad (4)$$

Where t is the pulling time (s), q is the heat flux, $MW/(m^2 \cdot k)$.

In the mould, the pulling time can also be expressed as $t=l/v$, so, equation (4) can be described as [16]:

$$q = 1.2 \times (2680 - 335 \times \sqrt{\frac{l}{v}}) \quad (5)$$

Where l is the distance from meniscus (m), v is the casting speed (m/s). Figure 4 shows the heat flux distribution along the height of mould with different casting speeds.

1.4 Computed parameters

Density, thermal conduction, specific heat, latent heat of fusion and mechanical properties as well as yield functions changing with temperature were developed [17, 18]. Regarding the thermal-expansion coefficient, temperature related computation model

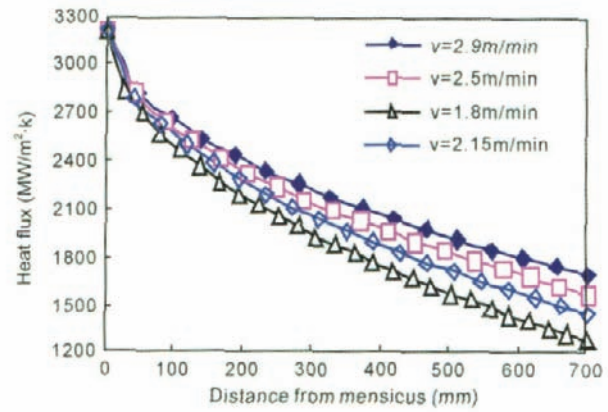


Fig. 4: Heat flux distribution along the height of mould

was specially established, with the influence of solid-liquid phase change well considered [19-21], the equation is shown as follow:

$$\alpha = \frac{\sqrt[3]{\frac{V}{V_{ref}}} - 1}{T - T_{ref}} \quad (6)$$

Where T is the present temperature ($^{\circ}C$), T_{ref} is the reference temperature ($^{\circ}C$), V is the present volume (m^3), V_{ref} is the reference volume (m^3); α is the linear expansion coefficient ($1/^{\circ}C$). The casting speed, carbon content, and pouring temperature etc. are shown in Table 1.

Table 1: Calculated steels and working conditions

Steels	Content of carbon (%)	Pouring temperature ($^{\circ}C$)	Liquidus ($^{\circ}C$)	Solidus ($^{\circ}C$)	Casting speed (m/min)
12CrMoV	0.125	1,536	1,513	1,470	2.9
X42	0.125	1,542	1,517	1,473	2.9
ST45EQ	0.165	1,531	1,511	1,465	2.5
37Mn5V	0.365	1,513	1,493	1,427	2.5
ER70S6	0.07	1,540	1,515	1,465	2.15
B72LX	0.72	1,492	1,472	1,372	1.8

2 Results and discussion

Two-dimensional model was applied to predict thermal-mechanical behavior of six different cast steel billets under different operating conditions. Fig. 5 shows the shrinkage contour at the mould exit with different time.

Just below the meniscus, steel solidifies against the mold and shrink away from the mould. The shrinkage of steel shell appears at 5 s, and then the shrinkage increases gradually and the shrinkage distribution becomes more uniform when compared with those at 5 s.

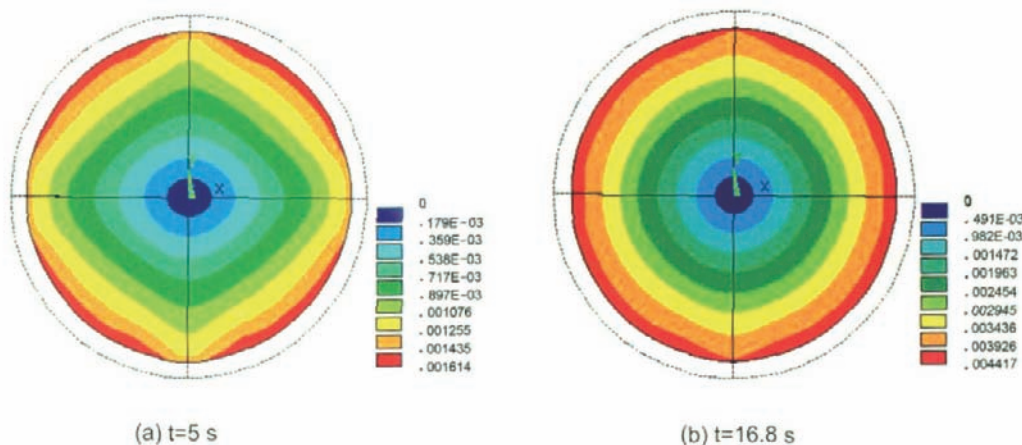


Fig.5: Round billet shrinkage contours of X42 at different time

Figure 6 shows the shrinkage distribution contours of the square B72LX steel billet at 10 s and 23.3 s (at the mould exit), Fig. 6(a) shows that the shrinkage at the corners and center of billet boundary is bigger than those at the off-corner positions. The shrinkage leads to the gap that forms between

the billet and mould plate. Figure 6(b) shows that the convex phenomenon of the boundary at the off-corner positions have decreased and the shrinkage value at boundary corner is more than those of the other boundary due to the intense cooling rate at the corner.

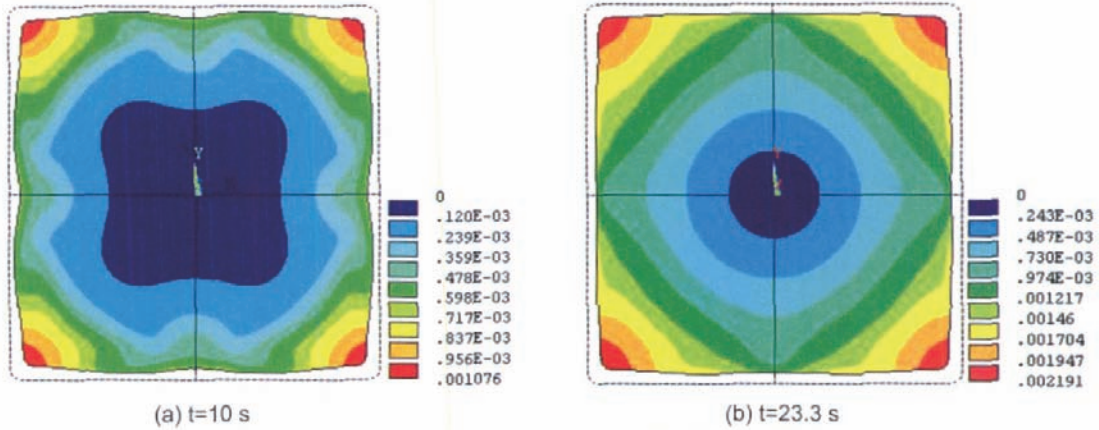


Fig. 6: Square billet shrinkage contours of B72LX at different time

Figure 7 shows the solidification shrinkage curves at point P along the height of the mould (four round billets of ST45EQ, 12CrMoV, X42 and 37Mn5V). Figure 8 shows the solidification shrinkage curves at the boundary center along the height of mould (two square billets of ER70S6 and B72LX). As shown in Fig. 7, it is obvious to see that the curves can be divided into three stages. At the first stage (0 mm to 150 mm), the solidified shell does not appear on

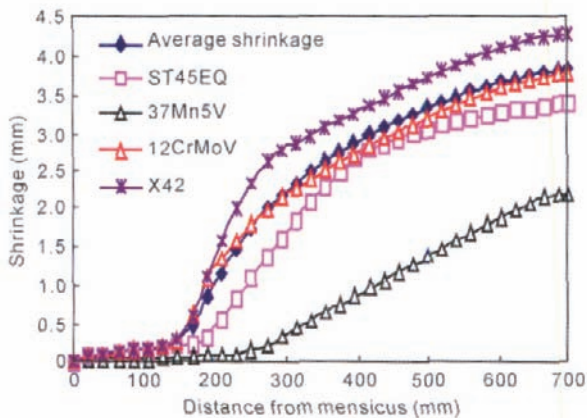


Fig. 7: Solidification shrinkage curves at point P in the round billets boundary along the height mould

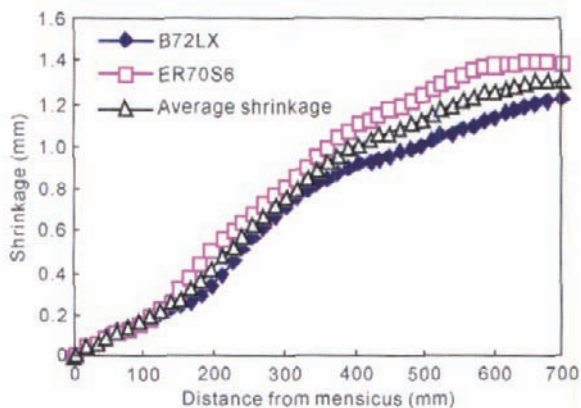


Fig. 8: Solidification shrinkage curves of square billets boundary center along the height of mould

the boundary of the billet, and the thickness of solid-liquid phase region is much thinner due to the release of latent heat of fusion, so the shrinkage is much smaller in this stage. More solidification occurs in the second stage (150 mm to 300 mm). The initially solidified shell contacts with the copper plate closely under the effect of ferrostatic pressure. Heat transfer efficiency is, therefore, improved. As a result, not only the solidified shell grew rapidly, the solid-liquid two phase region enlarging continuously also. Liquid phase shrinkage, solid-liquid two phase shrinkage and solid phase shrinkage in the cast billet accumulated together and result in the total shrinkage of the boundary. The shrinkage is most obvious in this stage. A relatively stable gap appears between the shell and copper plate at the third stage (over 300 mm). The heat transfer efficiency is reduced by the gap, so the accumulated effect of solidification shrinkage tends to become slow, but total shrinkage is increasing continuously. At the mould exit, the shrinkage of X42 steel is the largest in all the round billets (reaching 4.3 mm). On the contrary, the shrinkage of 37Mn5V steel is only 2.2 mm.

For 37Mn5V steel, it is different from the other three kinds of steels in carbon content, temperature region of solid-liquid phase and casting speed, therefore the shrinkage curve at point P has two obvious stages which are slightly different from others.

As shown in Fig. 8, the shrinkage in the square billets is obviously less than those in the round billets. The shrinkage of B72LX steel reaches 1.22 mm and ER70S6 steel is 1.38 mm at the mould exit. The square billets shrinkage can also be divided into three stages. The shrinkage curves of the two steels almost coincide with each other under the meniscus from 0 to 110 mm. From 110 mm to 390 mm, shrinkage increases quickly and the two curves are very close to each other. Shrinkage curves become gentle and total shrinkage keeps on increasing for over 390 mm, and the curves of the two steels billets are obviously different.

3 Mould taper optimization

The mould taper should be determined from the actual air gap, which can be obtained by combining the gaps mainly contributed by steel shrinkage and distortion. As known, the multiple or continuous taper mould should be adopted to decrease the gap width between the solidified shell and mould wall, so as to ensure good contact between the strand shell and the mould wall to maintain the heat flow rate and thus to

improve billet quality. The method for designing continuous taper in the mould is discussed below.

The solidification of steel obeys the solidification shrinkage curve (from numerical simulation results); the mould wall position should be tapered inwards with changing taper in the parabolic curve, in accordance with the actual solidified shell after shrinking in the mould. The inner cavity of mould with continuous parabolic taper is illustrated schematically in Figs. 9–11.

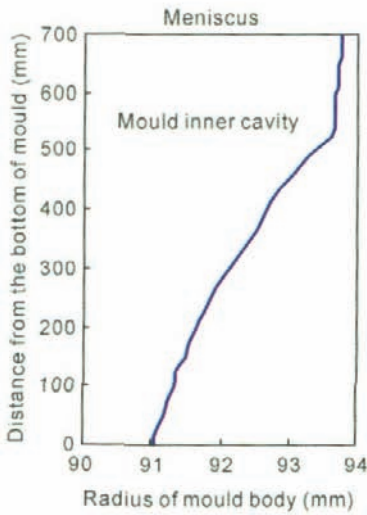


Fig. 9: Mould ideal taper of round billets (ST45EQ, 12CrMoV, X42)

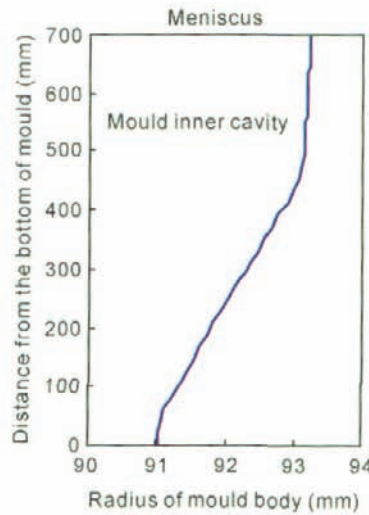


Fig. 10: Mould ideal taper of round billets (37Mn5V)

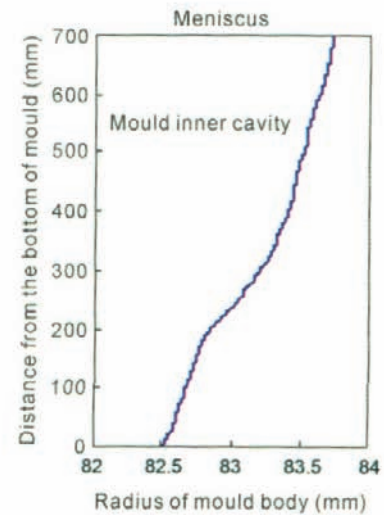


Fig. 11: Mould ideal taper of square billets (B72LX, ER70S6)

In the actual production, it is impossible to provide different moulds for each kind of steel. Based on the similarity of shrinkage curves of different steels, the average curves are parabolic-like, as shown in Fig. 7 and Fig. 8. Therefore, it is easy to design an ideal mould taper by only rotating the average curves with 90° which can be gained by similar curves of same billets, and they are basic foundation in the design and optimization of the mould taper. As for the 37Mn5V steel, its shrinkage curve has marked difference from the other steels, so a special mould taper was designed for it. The taper's ideal mould boundary is schematically shown in Figs. 9, 10 and 11. The longitudinal coordinates are distance from the mould bottom, and horizontal coordinates are the radiuses of mould body.

4 Experimental results

Based on the shrinkage curves in the mould, the continuous parabolic taper moulds were designed and produced by the factory. The experimental data was gained by using of the designed moulds under industrial conditions. The round mould was used to investigate the lifetime of the designed mould, and the lifetime reached at 322 heats, higher than the factory's requirements and more than the lifetime of the imported mould, which reaches to 200 heats only. The square mould has been worked for 55 heats without any problem. The test has not yet been finished because there is no further production task. Therefore, the real lifetime of the square mould is not

clearly known. Table 2 shows the lifetime test results of the designed mould obtained by factory.

Table 2: Lifetime test results of the designed mould

Items	Round mould	Square mould
Total number of heats	322	55
Pouring times	24	6
Max continuous cast heats	47	22
Average continuous cast heats	13.4	9.2
Steel species	35	9

Table 3 and Table 4 show the quality analysis of round and square billets, the 2nd strand moulds are the designed round and square moulds, and the others are the compared moulds.

In Table 3, surface crack, center crack and center porosity, do not appear in all the billets. The crystallization structures above class 3 appear to some extent for all the cases, but the crystallization structures of the 2nd strand are better than other strand. The surface cracks emerge in the 1st and 6th strand only. In Table 4, the surface crack and the center crack do not appear in all experimental strand, but the center porosity and crystallization structure above grade 3 appear in the billets. Comparing with the other experimental strand, the crystallization structure and the center porosity of the 2nd run are better, or equivalent. It also shows that the surface crack does not appear in the billets in all cases.

Table 3: The quality analysis of the round billets in the designed mould

Technical requirement of criterion	Internal quality				Surface quality
	Subsurface crack ≥1 class (%)	Center crack ≥1 class (%)	Center porosity ≥2 class (%)	Crystallization structure ≥3 class (%)	Surface crack Ratio of crack
1st strand	0	0	0	48	0.41%
2nd strand	0	0	0	32	0.00%
3rd strand	0	0	0	37	0.00%
4th strand	0	0	0	44	0.00%
5th strand	0	0	0	36	0.00%
6th strand	0	0	0	53.3	0.08%

Table 4: The quality analysis of the square billets in the designed mould

Technical requirement of criterion	Internal quality				Surface quality
	Subsurface crack ≥1 class (%)	Center crack ≥1 class (%)	Center porosity ≥2 class (%)	Crystallization structure ≥3 class (%)	Surface crack Ratio of crack
1st strand	0	0	17	62.3	0.00%
2nd strand	0	0	21	50	0.00%
3rd strand	0	0	19	69.3	0.00%
4th strand	0	0	16	79.3	0.00%
5th strand	0	0	17	73	0.00%

5 Conclusions

(1) At the mould exit, the average shrinkage of round billets (ST45EQ, 12CrMoV and X42) reaches at 3.8 mm and the average shrinkage of square billets (ER70S6 and B72LX) reaches at 1.3 mm for the center of the boundary.

(2) According to the simulated shrinkage curve, the round mould for ST45EQ, 12CrMoV, X42 (low carbon steel) can be designed by three continuous parabolic tapers, and 37Mn5V (high carbon steel) can be designed by two continuous parabolic tapers. Square mould for the B72LX and ER70S6 steel billets can be designed by three continuous parabolic taper, because their shrinkage curves have similar tendency.

(3) The lifetime of the designed mould satisfied with the factory's requirement. Compared with the imported moulds, the designed moulds have equivalent lifetime and even better.

References

- [1] Cao Yuanfeng, Zhang Yongxing, Xu Baosheng, et al. Research on the billet casting mold. *Steel Making*, 1997, (13): 48–52. (in Chinese)
- [2] Cai Kaike. *Pouring and Solidification*. Beijing: Metallurgical Industry Press, 1987. (in Chinese)
- [3] Jin Junze, Zheng Xianshu, Guo Keren, et al. Computer simulation of the solidification in billet continuous casting. *Iron and Steel*, 1985, 20: 19–27. (in Chinese)
- [4] Thomas B G, Li G, Moitra A, et al. Analysis of Thermal and Mechanical Behavior of Copper Molds during Continuous Casting of Steel Slabs. *Proc. 80th Steelmaking Conference*. Chicago, USA, ISS Herty Award, 1997, 1–19.
- [5] Park J K, Samarasekera I V, Thomas B G. Analysis of Thermal and Mechanical Behavior of Copper Molds during Thin slab Casting. *Proc. 83th Steelmaking Conference*. Pittsburgh, USA, Iron and Steel Society, 2000: 9–21.
- [6] Wang Engang, He Jicheng, et al. Finite element analysis of thermal elasto-plastic stress on the continuous casting billet in mold. *Journal of Northeastern University (Natural Science)*, 1998, 19(6): 555–557. (in Chinese)
- [7] Risso J M, Huespe A E, Cardona A. Thermal stress evaluation in the continuous casting process. *Int. J. Number. Meth. Engng*, 2006, 65: 1355–1377.
- [8] Thomas G Oconnor and Jonathan A Dantzig. Modeling the thin-slab continuous-casting mold. *Metallurgical and Materials Transactions B*, 1994, 25(3): 443–457.
- [9] Wang Baofeng, Ding Gguo, Zhang Jianguo, et al. Optimum of mould taper design for slab casting of austenite stainless steel. *Special Steel*, 2005, 26(2): 38–40. (in Chinese)
- [10] Zhu L G, Kumar R V. Modeling of steel shrinkage and optimization of mould taper for high speed continuous casting. *Ironmaking and Steelmaking*, 2002, 29(1): 61–69.
- [11] Chow C, Samarasekera I V, Walker B N. High speed continuous casting of steel billets Part 2: Mould heat transfer and mould design. *Ironmaking and Steelmaking*, 2007, 34(1): 76–82.
- [12] Yang Bingjian. Modeling temperature stress distributions in continuously cast steel slab. *Foundry Technology*, 1991(2): 45–48. (in Chinese)
- [13] Janik M, Dyja H, Berski S, Banaszek G. Two-dimensional thermo-mechanical analysis of continuous casting process. *Journal of Materials Processing Technology*, 2004: 578–582.
- [14] Wang Engang, He Jicheng, Yang Zekuan, et al. Finite element numerical simulation on solidification and stress of continuous casting billet in mold. *Acta Metallurgica Sinica*, 1999, 35(4): 433–438.

- [15] Sheng Yiping, Kong Xiangdong, Yang Yongli. Study on Thermal Boundary Conditions in the Mold Continuous Casting. *Chinese Journal of Mechanical Engineering*, 2007, 18(13): 1615–1618. (in Chinese)
- [16] Kang Li, Wang Engang, He Jicheng. Numerical Simulation on deformation and temperature field of continuous casting mould. *Journal of Materials and Metallurgy*, 2006, 5(3):190–194. (in Chinese)
- [17] Kelly J E, O'Connor T G, Thomas B G. Initial Development of Thermal and Stress Fields in Continuously Cast Steel Billets. *Metallurgical Transaction A*, 1988, 19 A: 2589–2602.
- [18] Yin Hebin. Analysis of thermo-mechanical behaviors in the mould for small round billet continuous casting. Dalian, Dalian University of Technology, 2005. (in Chinese)
- [19] Li C S, Thomas B G. Thermomechanical Finite-Element Model of Shell Behavior in Continuous Casting of Steel. *Metallurgical and Materials Transaction B*, 2004, 35B: 1151–1172.
- [20] Koric Seid, Thomas B G. Thermo-mechanical models of steel solidification based on two elastic visco-plastic constitutive laws. *Journal of Materials Processing Technology*, 2008, 197(1-3): 408–418.
- [21] Chandra S, Brimacombe J K, Samarasekera I V. Mould-strand interaction in continuous casting of steel billets. *Ironmaking and Steelmaking*, 1993, 20(2): 104–112.

The project is financially supported by National Natural Science Foundation of China (No.50601003 and No.50971032), and New Century Excellent Talents in University (NCET-07-0137), and Scientific Research Fund of Liaoning Provincial Education Department .